

# 3D Tomography from Few Projections in Experimental Fluid Dynamics

Stefania Petra, Andreas Schröder and Christoph Schnörr

**Abstract** We study the tomographic problem of reconstructing particle volume functions in experimental fluid dynamics from the general viewpoint of compressed sensing, which is a central theme of current research in applied mathematics. The probability of exact reconstructions from few projections is studied empirically and shown to resemble provable results for idealized mathematical measurement setups. Application of our reconstruction algorithm to noisy projections outperforms the state-of-the-art both with respect to accuracy and runtime.

## 1 Introduction

This paper summarizes results of our project that has started two years ago. Our research work is motivated by the work [10]. The authors introduced a new 3D technique, called *Tomographic Particle Image Velocimetry (TomoPIV)* for imaging turbulent fluids with high speed cameras. The technique is based on the instantaneous reconstructions of particle volume functions from few and simultaneous projections (2D images) of the tracer particles within the fluid. The reconstruction of the 3D image from 2D images employs a standard algebraic reconstruction algorithm [11].

Tomographical setups relevant for experimental fluid dynamics significantly differ from those of medical imaging, where projections of the object to be reconstructed are acquired under a large range of angles, i.e. the image to be reconstructed is highly oversampled, while reconstruction algorithms are based on the regularization of the inverse Radon transform [15]. TomoPIV, on the other hand, employs only few projections due to both limited optical access to wind and water tunnels and cost

---

S. Petra, C. Schnörr  
University of Heidelberg, Dept. Math. and Computer Science, Image and Pattern Analysis Group,  
{petra,schnoerr}@math.uni-heidelberg.de

A. Schröder  
German Aerospace Center (DLR), Göttingen, andreas.schroeder@dlr.de

and complexity of the necessary measurement apparatus. As a consequence, the reconstruction problem becomes severely ill-posed, and both the mathematical analysis and the design of algorithms fundamentally differ from the standard scenarios of medical imaging.

Our research work addresses two major open problems:

1. A crucial parameter for 3D fluid flow estimation from image measurements is particle density. This parameter also largely influences the tomographical reconstruction problem. Higher densities ease subsequent flow estimation by means of a *cross correlation technique* [19] and increase the resolution and measurement accuracy. However, higher densities also aggravate ill-posedness of the reconstruction problem. A thorough investigation of this trade-off is lacking.
2. Another major issue concerns problem size and computation time. 3D problems and, in particular, time-dependent 3D problems require considerable computational resources. Yet, adopting some ad hoc iterative reconstruction algorithm and terminating after few, sometimes even after a single(!) iteration, cannot be regarded as a solid strategy without further analysis of the setup and its essential parameters. A study of the reconstruction problem – optimization criteria and algorithms – helps to underpin proper design of technical systems.

The objective of our project is to address these two problems taking into account relevant developments in applied mathematics.

## 2 Related Work

**TomopIV** [10] adopts a simple discretized model for an image-reconstruction problem known as the *algebraic image reconstruction* model [6], which assumes that the image consists of an array of unknowns (voxels), and sets up algebraic equations for the unknowns in terms of measured projection data. The latter are the pixel entries in the recorded 2D images that represent the integration of the 3D light intensity distribution  $I(z)$  along the pixels line-of-sight  $L_i$  obtained from a calibration procedure. We consider an alternative to the classical voxel discretization and assume that the image  $I$  to be reconstructed can be approximated by a linear combination of Gaussian-type *basis functions*  $\mathcal{B}_j$ ,

$$I(z) \approx \sum_{j=1}^n x_j \mathcal{B}_j(z), \quad \forall z \in \Omega \subset \mathbb{R}^3, \quad \text{of the form}$$

$$\mathcal{B}_j(z) = e^{-\frac{\|z-p_j\|_2^2}{2\sigma^2}}, \quad \text{for } z \in \mathbb{R}^3 : \|z-p_j\|_2 \leq r,$$

or value 0, if  $\|z-p_j\|_2 > r$ , located at a Cartesian equidistant 3D grid  $p_j$ ,  $j = 1, \dots, n$  within the volume of interest  $\Omega$ . The choice of a Gaussian-type basis function is justified in the TomopIV setting, since a particle projection in all directions results in a so-called *diffraction spot* of approximately 3 pixel diameter. The  $i$ -th measurement

obeys

$$b_i := \int_{L_i} I(z) dz \approx \sum_{j=1}^n x_j \int_{L_i} \mathcal{B}_j(z) dz = \sum_{j=1}^n x_j a_{ij},$$

where  $a_{ij}$  is the value of the  $i$ -th pixel if the object to be reconstructed is the  $j$ -th basis function. The main task is to estimate the weights  $x_j$  from the recorded 2D images, corresponding to basis functions and solve  $Ax \approx b$ .

The matrix  $A$  has dimensions (# pixel =:  $m$ )  $\times$  (# basis functions =  $n$ ). Since each row indicates those basis functions whose support intersect with the corresponding projection ray the projection matrix  $A$  will be sparse. Unfortunately there is no sparsity pattern which can be exploited.

**Compressed sensing** is a new measurement paradigm [3, 8] which seeks to capture the "essential" aspects of a high-dimensional object using as few measurements as possible. The basic principle is that sparse or compressible signals (i.e. can be well approximated with a small number of active basis functions) can be reconstructed *exactly* from a surprisingly small number of linear measurements, provided that the measurements satisfy an *incoherence* property (see, e.g. [5] for an explanation of incoherence).

A further remarkable result of Candès and Tao [4] is that if, for example, the rows of  $A$  are randomly chosen Gaussian distributed vectors, there is a constant  $C$  such that for a signal  $x$  with at most  $k$  nonzero entries and  $m \geq Ck \log(\frac{n}{k})$ , the solution  $x^*$  of

$$\min \|x\|_1 \text{ s.t. } Ax = b \quad (1)$$

will be exactly the original signal  $x$  with overwhelming probability.

Donoho and Tanner [9] have computed sharp reconstruction thresholds for Gaussian measurements, such that for any choice of sparsity  $k$  and signal size  $n$ , the required number of measurements  $m$  to recover  $x$  can be determined precisely.

Within our particular TomoPIV setting the size of  $x$  can be chosen arbitrarily large depending on the number of gridpoints where the basis functions are located, e.g.  $n = O(10^9)$ . The current measurement apparatus employs 4-6 camera of  $1024^2$  pixels each. The particle density is 0.05pp (particle/pixel), thus the underlying signal should be well approximated by  $O(k)$  Gaussian basis functions, where  $k = 0.05 \cdot 1024^2$ . For a perfectly  $k$  compressible signal  $k \log(\frac{n}{k}) = 4.3609 \cdot 10^5$  pixels would suffice, which corresponds to half of the number of pixels in one camera. Why are then still 4-6 camera currently in use? One answer is that the signal is only approximately  $27 \cdot 0.05 \cdot 1024^2$  sparse when the 3D image is discretized in voxels in view of one particle diameter of 3 voxels. This corresponds to at least  $7.1089 \cdot 10^6$  measurements (7 cameras) to obtain perfect recovery of the 500000 particles within the volume. Moreover, the measurement matrix  $A$  lacks the nice properties as incoherence which would guarantee perfect recovery, see [17] for a discussion on both voxel- and blob-based discretization scenarios. However the blob-based projection matrix yields considerably better reconstruction of a  $k$ -sparse vector due to the fact that each basis function is intersected by more pixel "rays", a property relevant for the deterministic measurement matrix construction from [12].

### 3 Reconstruction Algorithms

#### 3.1 Algebraic reconstruction techniques

The state-of-the-art of TomoPIV [10] is the *Multiplicative Algebraic Reconstruction Technique (MART)*. It was first proposed in [11] and is a *maximum entropy* algorithm, with a solution satisfying

$$\min f_E(x) := \sum_i x_i \log(x_i) \quad \text{s.t. } Ax = b, x \geq 0.$$

It applies only to systems in which  $b > 0$  and  $A$  has only nonnegative entries. This applies to our scenario since all  $a_{ij} > 0$  and zero or negligible measurements can be eliminated by a procedure leading to an "equivalent" feasible set  $\mathcal{F}_r$  of reduced dimensionality, see [17, Prop. 2.1]. The authors in [2] proposed a further noticeable preprocessing procedure called *multiplicative line-of-sight estimation* to fix possible particle positions and thus to reduce considerably the dimension of the original system. MART converges linearly to a solution in  $\mathcal{F}_r$  provided that it is nonempty, compare [16] and the reference therein.

The closely related *Simultaneous Multiplicative Algebraic Reconstruction Technique (SMART)* minimizes the Kullback-Leibler cross entropy  $KL(Ax, y)$  over the nonnegative orthant and converges, for consistent projection equations, to that member of  $\mathcal{F}_r$  for which the cross-entropy distance to the initial vector  $KL(x, x_0)$  is minimized.

The iterative method *SART (Simultaneous Algebraic Reconstruction Technique)* of Andersen and Kak, see [1], was successfully applied to tomographic particle image reconstruction in [2]. SART writes as

$$x^{k+1} = x^k + \lambda VA^T W(b - Ax^k),$$

where  $\lambda \in (0, 2)$ ,  $V$  and  $W$  diagonal matrices defined by

$$V := \text{diag}\left(\frac{1}{A_{+1}}, \dots, \frac{1}{A_{+n}}\right) \quad \text{and} \quad W := \text{diag}\left(\frac{1}{A_{1+}}, \dots, \frac{1}{A_{m+}}\right)$$

with  $A_{+j} := \sum_{i=1}^m a_{ij}$  and  $A_{i+} := \sum_{j=1}^n a_{ij}$ . SART was developed as a major refinement of the *Algebraic Reconstruction Technique (ART)* [11], a reincarnation of Kaczmarz's [14] method of alternating projections. The convergence of SART towards a solution of the weighted least squares problem  $\min \|W^{\frac{1}{2}}(Ax - b)\|$  was established in [13]. The likewise parallelizable method due to Cimmino was recently reconsidered by the authors [18] in the context of TomoPIV.

All the methods above have the distinctive feature that they are *row action method* [6] and have demonstrated effectiveness on huge problem instances but suffer from the slow convergence rate.

They return a sufficiently good approximation  $x^k$  after few iterations [10, 2] for sufficiently small particle densities. In practice, subsequent iterations do not improve

the quality of the computed solution, however, but actually result in increasingly worse approximations. This is because the iterates become completely dominated by the errors inevitably present in the data.

### 3.2 $\ell_1$ -minimization and Linear Programming

The  $\ell_1$ -minimization problem (1), known also as *basis pursuit* [7], can be recast as a linear program and then solved by conventional linear programming solvers. However, such solvers are not suited for large-scale matrices  $A$  arising in our application. Usually only matrix-vector operations involving  $A$  and  $A^T$  are feasible. A recent method motivated by the compressed sensing context is the *Bregman Iterative Algorithm* [20]. The name is due to the fact that it employs a Bregman iterative regularization, which gives an accurate solution after solving only a very small number of instances of the unconstrained problem

$$\min_x \|x\|_1 + \frac{1}{2} \|Ax - b^k\|_2^2$$

by a fast *fixed-point continuation (FPC)* solver that is based solely on simple operations for solving the above unconstrained subproblem. The algorithm starts with the initialization  $b^0 := 0$ ,  $x^0 := 0$  and then for  $k = 0, 1, \dots$  writes

$$\begin{aligned} b^{k+1} &:= b^k + (b^k - Ax^k), \\ x^{k+1} &:= \operatorname{argmin}_x \|x\|_1 + \frac{1}{2} \|Ax - b^{k+1}\|_2^2. \end{aligned}$$

It is equivalent to the well-known augmented Lagrangian method (also known as the method of multipliers), thus constraints can also be included. It is shown in [20] that the method yields a global optimum in a finite number of iterations.

## 4 Design and Evaluation Criteria

### 4.1 Design Criteria

Assuming there could be several possible solutions, the common practice is the definition of an optimization problem of the form

$$\min f(x) \text{ s.t. } Ax = b, [x \geq 0,]$$

where  $f$  measures the quality of the candidate solutions. Possible choices for this penalty could be:

- entropy measures as in the case of MART and SMART, respectively.

- $\ell_p$ -norms for various  $p$  in the range  $[0, \infty)$ . Popular choices are:
  - $\ell_2$ -minimization is the method of least squares. It finds out of all possible solutions the one of least energy and can be easily carried out (e.g. ART, Cimmino). Unfortunately, this minimizer is not guaranteed at all to be sparse. If we take nonnegativity into account this situation may change dramatically.
  - $\ell_1$ -minimization is convex and can be solved in reasonable time by convex programming techniques. The important question in this connection is whether the method actually can recover the original  $k$ -sparse signal  $x$ .
  - $\ell_0$ -minimization enforces sparsity and selects out of all possible solutions which match the given data the sparsest one. This regularization approach was considered by the authors in [18] in the context of TomoPIV, but appears to be less practical in the real TomoPIV setting because several(!) linear programs for one volume reconstruction have to be solved.

We discussed above (compressed sensing) that the choices  $p = 0$  and  $p = 1$  may lead to the same reconstruction provided it is sparse enough. This equivalence phenomenon depends on properties of the measurements matrix  $A$ . They are known for classes of matrices none of which covers our application area, however.

Clearly, if the set of feasible solutions  $\mathcal{F} := \{x | Ax = b, x \geq 0\}$  contains only a single element, then all the above choices of  $f$  will lead to the same solution. This is exactly what happens when a sufficiently sparse solution exists. In this case we can apply any efficient method designed to find the element in  $\mathcal{F}$ .

## 4.2 Evaluation Criteria

We wish to inspect empirical bounds on the required sparsity that guarantee exact reconstruction and critical parameter values that yield a performance similar to the settings considered in compressed sensing (e.g. [9]).

These parameter values allow us to answer the question how sparse a vector should be (particle density) such that  $\ell_0$  can be solved by  $\ell_1$ -minimization, linear programming or quadratic programming with constraints.

Consider a matrix  $A \in \mathbb{R}^{m \times n}$ , the undersampling ratio  $\delta = \frac{m}{n} \in (0, 1)$  and the sparsity as a fraction of  $m$ ,  $k = \rho m$ , for  $\rho \in (0, 1)$ . This phase transition  $\rho(\delta)$  as function of  $\delta$  indicates the necessary undersampling ratio  $\delta$  to recover a  $k$ -sparse solution with overwhelming probability. More precisely, if  $\|x\|_0 \leq \rho(\delta) \cdot m$ , then with overwhelming probability the  $\ell_0$ -problem of finding the  $k$ -sparsest solution can be solved by  $\ell_1$ -minimization. For Gaussian matrices there are precise values of  $\rho(\delta)$ , see [9], which can be computed analytically.

Relevant for TomoPIV is the setting as  $\delta \rightarrow 0$  and  $n \rightarrow \infty$ , that is severe undersampling. Then a *strong asymptotic threshold*  $\rho_S(\delta) \approx (2e \log(1/\delta))^{-1}$  and *weak asymptotic threshold*  $\rho_W(\delta) \approx (2 \log(1/\delta))^{-1}$  holds for Gaussian matrices. The weak threshold says that  $\ell_0/\ell_1$ -equivalence typically holds while for the strong one equivalence holds for all  $\rho_S(\delta) \cdot m$ -sparse signals.

## 5 Numerical Results

Although the projection matrices within the TomoPIV setting do not satisfy the nice properties of Gaussian measurement matrices, we observed critical parameter values similar to those for Gaussian matrices. We generated a  $100 \times 20$  grid at which we located  $n = 2000$  Gaussian basis functions. First a big projection matrix was generated resulting from parallel projections at angles  $(-60^\circ, -55^\circ, \dots, 0^\circ, 5, 10, \dots, 60^\circ)$ . Then  $m = \delta n$  random rows were selected to compute the right hand side measurement vector. The plane  $(\delta, \rho) = [0, 0.7] \times [0, 1]$  was divided in a  $20 \times 20$  mesh, and for each point 50 random problem instances were generated. The empirical probability that the approaches presented above correctly recover a  $k = \rho m$ -sparse solution for each parameter combination is presented in Fig. 1 (a), (c)-(f). For the asymptotic scenario see Fig. 1 (b), computed for the bigger value  $n = 200000$ . A threshold-effect is clearly visible in all figures exhibiting parameter regions where the probability of exact reconstruction is close to one.

The advantage of using blob-based volume discretizations is demonstrated in Figure 2. Figure 3, finally, illustrates the comparison of our approach with the SART iteration used in [2].

## 6 Conclusions

The reconstruction of a relatively dense particle distribution in a volume from few projections can be modeled as finding the sparsest solution of an underdetermined linear system of equations, because the original particle distribution can be well approximated with only a very small number of active basis functions relative to the number of possible particle positions in a 3D domain. In general the search for the sparsest solution is intractable (NP-hard), however. The newly developed theory of Compressed Sensing showed that one can compute via  $\ell_1$ -minimization or linear programming the sparsest solution for underdetermined systems of equations provided they satisfy certain properties, which unfortunately do not hold for our particular scenario. Still, we showed empirically in the present work that there are thresholds on sparsity (i.e. density of the particles) depending on the numbers of measurements (recording pixel in the CCD arrays), below which these methods will succeed and above which they fail with high probability. When they succeed they yield near perfect reconstructions (without any ghost-particles). Theoretically, constrained versions of several algebraic reconstructions techniques will also converge to the original solution for very sparse scenarios. Due to their slow convergence they are outperformed by an augmented Lagrangian method for  $\ell_1$ -minimization, however, that provides considerably better particle reconstructions than the currently used methods.

**Acknowledgements** The authors would like to thank the German Science Foundation (DFG) for supporting this work within the priority research program 1147, "Image Measurements in Ex-

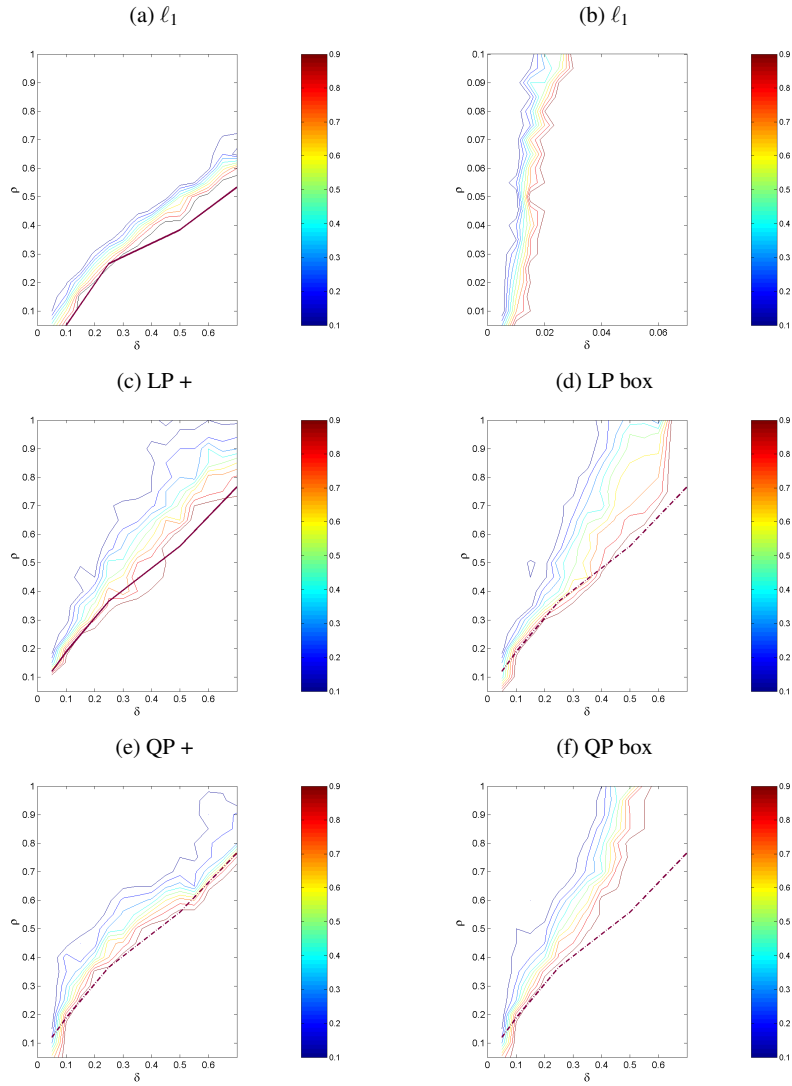


**Fig. 1** Probability of correct recovery of a random particle distribution that can be expressed with exactly  $k$  basis functions as a function of  $\delta = \frac{m}{n}$ ,  $n = 2000$  and  $k = \rho m$ . The thick curve  $\rho(\delta)$  depicts a phase transition of  $\ell_1$ -minimization (a) and linear programming (c)-(f) to find the  $k$ -sparsest solution, but for Gaussian random matrices, see [9]. Figure (b) shows a "zoom in" of (a): here we have chosen  $n = 200000$ . We believe that  $\rho(\delta) \approx |2\log(C\delta)|^{-1}$  as  $\delta \rightarrow 0$  similar to the analytic curve for Gaussian matrices presented in [9]. The right  $n$ -dependent value of constant  $C$  is a subject of our current research.

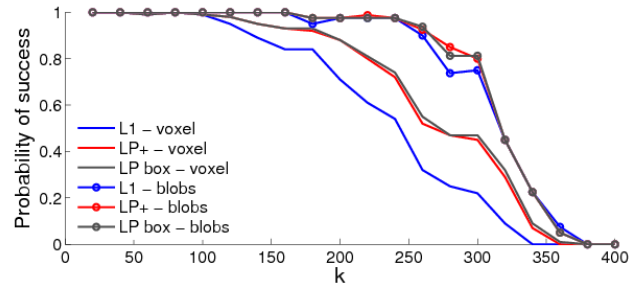


**Fig. 2** Empirical probability of exact reconstruction of an increasing number  $k$  of "particles" by means of an  $3 \cdot 32^2 \times 32^3$  projection matrix from 3 orthogonal projections for both voxel and blob scenarios. Substantially more particles are reconstructed for the blobs-based discretization matrix for all three methods of choice:  $\ell_1$ -minimization (blue), linear programming with positivity constraints only (red), linear programming with box constraints (black).

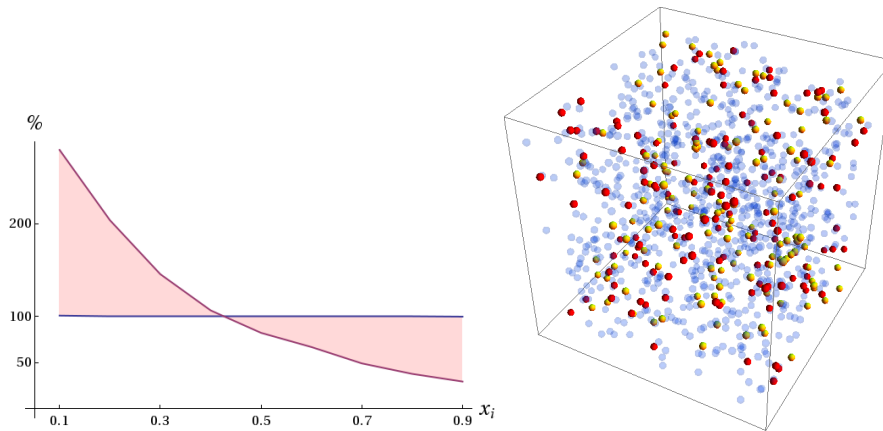


**Fig. 3** Reconstruction experiment for 1000 particles in a small cube from 3 orthogonal projections, using SART reconstruction after reducing the system (cf. section 3.1) and the Bregman iterative algorithm (section 3.2). The iteration was terminated after convergence for the latter algorithm, and after a comparable runtime for SART. **Left panel.** Number of reconstructed particles corresponding to the coefficients  $x_i$  exceeding a threshold  $\in [0.1, 0.9]$  for SART (red) and our approach (blue). SART may return far too many particles ( $> 200\%$ ) or too less, whereas our approach always returned the exact reconstruction. **Right panel.** Choosing a threshold for which SART returns the correct number of particles yields both missing particles (yellow) and additional ghost particles (red).

perimental Fluid Mechanics”, under grant SCHN 457/10-1. The authors enjoyed collaboration, fruitful discussions and data exchange with many partners of the priority program, including Volker Beushausen, Christoph Brücker, Octavian Frederich, Christoph Garbe, Rainer Hain, Bernd Jähne, Christian Kähler, Hans-Gerd Maas, Wolfgang Nitsche, Holger Nobach, Torsten Putze, Frank Thiele, Cam Tropea, and Rüdiger Westermann.

## References

1. Andersen A, Kak A (1984) Simultaneous Algebraic Reconstruction Technique (SART): A Superior Implementation of ART, *Ultrasonic Imaging*, 6:81–94.
2. Atkinson CH, Dillon-Gibbons CJ, Herpin S, Soria J (2008) Reconstruction Techniques for Tomographic PIV (Tomo-PIV) of a Turbulent Boundary Layer, In: 14th Int Symp on Applications of Laser Techniques to Fluid Mechanics, Lisbon
3. Candès E, Romberg J, Tao T (2006) Robust uncertainty principles: Exact signal reconstruction from highly incomplete frequency information, *IEEE Trans on Information Theory*, 52:489–509
4. Candès E, Tao T (2006) Near optimal signal recovery from random projections: Universal encoding strategies?, *IEEE Trans on Information Theory*, 52:5406–5425
5. Candès E, Romberg J (2007) Sparsity and incoherence in compressive sampling, *Inverse Problems*, 23:969–985
6. Censor Y, Zenios SA (1997) *Parallel Optimization: Theory, Algorithms and Applications*, Oxford University Press, New York
7. Chen SS, Donoho D, Saunders MA (1998) Atomic decomposition by basis pursuit, *SIAM J Sci Comput* 20:33–61
8. Donoho D (2006) Compressed sensing, *IEEE Trans on Information Theory* 52:1289–1306
9. Donoho D, Tanner J (2006) Thresholds for the recovery of sparse solutions via ell-1 minimization, *Conf on Information Sciences and Systems*
10. Elsinga G, Scarano F, Wieneke B, B van Oudheusden (2006) Tomographic particle image velocimetry, *Exp Fluids* 41:933–947
11. Gordon R, Bender R, Herman GT (1970) Algebraic reconstruction techniques (ART) for three-dimensional electron microscopy and X-ray photography, *J Theor Biol* 29:471–481
12. Indyk P (2008) Explicit constructions for compressed sensing of sparse signals, *Symp on Discrete Algorithms*
13. Jiang M, Wang G (2001) Convergence of the simultaneous algebraic reconstruction technique (SART), *IEEE Trans on Image Processing*, 12:957–961
14. Kaczmarz S (1937) Angenäherte Auflösung von Systemen linearer Gleichungen, *Bull Acad Polonaise Sci et Lettres A*:355–357.
15. Natterer F, Wübbeling F (2001) *Mathematical Methods in Image Reconstruction*, SIAM
16. Petra S, Schnörr C, Schröder A, Wieneke B (2007) Tomographic Image Reconstruction in Experimental Fluid Dynamics: Synopsis and Problems, In: *Mathematical Modelling of Environmental and Life Sciences Problems*, Ed Acad Romane, Bucuresti
17. Petra S, Schröder A, Wieneke B, Schnörr C (2008) On Sparsity Maximization in Tomographic Particle Image Reconstruction, In: *Pattern Recognition – 30th DAGM Symposium*, vol 5096 of LNCS, Springer Verlag
18. Petra S, Popa C, Schnörr C (2008) Extended and Constrained Cimmino-type Algorithms with Applications in Tomographic Image Reconstruction, IWR preprint, <http://www.uni-heidelberg.de/archiv/8798/>
19. Scarano F, Riethmüller ML (2000) Advances in iterative multigrid PIV image processing, *Exp Fluids* 29:51–60
20. Yin W, Osher S, Goldfarb D, Darbon J (2008) Bregman Iterative Algorithms for l1-Minimization with Applications to Compressed Sensing, *SIAM J Imaging Sciences* 1:143–168